HYDROMECHANICS OF WIND-ASSISTED SHIP PROPULSION
VERIFICATION OF RANS METHODOLOGY

N.J. van der Kolk*, J.A. Keuning† and R.H.M. Huijsmans‡

*TU Delft,
Mekelweg 2, 2628 CD Delft
The Netherlands
e-mail: n.j.vanderkolk@tudelft.nl

Final version published in: Ocean Engineering Volume 201, 1 April 2020, 107024
DOI: 10.1016/j.oceaneng.2020.107024

ABSTRACT

Wind energy as an auxiliary form of propulsion for commercial ships has again become of great interest as a possible response to volatile fuel prices and increasingly stringent environmental regulations. A well-founded performance prediction tool is a key prerequisite for the further development of this promising technology, and with the support of the European Commission and others, a group of researchers at Delft University of Technology is developing a performance prediction program for these hybrid ships. Reynolds-Averaged Navier Stokes (RANS) packages will be one of the primary tools used during the study. The advent of the numerical towing tank brings possibilities but also new challenges. The predominance of large, separated flow structures in the wake of the sailing ship, and the particular interest in the transverse force component points to a conscientious grid verification. Here, it is sufficient to achieve parity for absolute uncertainty within the larger context of the project.

INTRODUCTION

Wind energy as an auxiliary form of propulsion for commercial ships has again become of great interest as a possible response to volatile fuel prices and increasingly stringent environmental regulations. A well-founded performance prediction tool is a key prerequisite for the further development of this promising technology, and with the support of the European Commission and others, a group of researchers at Delft University of Technology is developing a performance prediction program for these hybrid ships. The Wind-Assisted Ship Propulsion (WASP) performance prediction tool will provide designers the ability to explore the possibilities offered by wind as an auxiliary propulsor. The aim is to deliver a regression-based force model that is applicable to a broad range of vessels. The WASP performance prediction program will allow for parametric investigations, and eventually for the optimization of commercial hull forms for sailing. The expansion and refinement of the force models is the subject of ongoing work at Delft University of Technology.

In the service of regression analysis, the Reynolds-averaged Navier Stokes (RANS) package FINE/Marine is used to assess hull variants. Simulation verification for integrated quantities on the bare-hull at model scale will be described here. The large, separated flow structures in

the wake of the sailing ship, and the particular interest in the transverse force has complicated the verification process; in discerning between (perhaps substantial) modelling errors and numerical errors. Taking the larger view, the sideforce is a central component in the larger evaluation for the performance of a wind-assist vessel. The uncertainty level for the prediction of sideforce should reflect the large impact of this component on the fidelity of the performance prediction.

Sailing Preliminaries

Fitting a commercial vessel with an auxiliary wind propulsor will introduce a set of forces and moments besides the desired aerodynamics thrust. The ship will sail with a leeway angle β about the yaw axis, equivalent to the angle of attack for the hull, in order to generate the hydrodynamic reaction in opposition to the transverse component of the aerodynamic force. Further, the distribution of the hydrodynamic sideforce along the hull may result in a net yaw moment. At last, the vertical separation between the sideforce components will create a heeling moment. As hybrid vessels, the performance of a wind-assist concept will depend on the contribution of the wind propulsor, alongside the efficiency of the conventional propulsion system and the drag penalty associated with heel and leeway: the “sailing condition”. Of course, the introduction of a sail-plan will only benefit the vessel if the net thrust gained outweighs any loss in efficiency or increase in resistance.

RANS CFD VERIFICATION PROCEEDURES

Methodology

Several governing bodies publish standards for simulation verification, including the International Towing Tank Committee (ITTC) [1] and the American Society of Mechanical Engineers (ASME) [2]. The Grid Convergence Index (GCI) of Roach is commonly accepted, thanks in part to his strong advocacy for standardization of Journal policies regarding uncertainty reporting for computational fluid dynamics. His influence is seen throughout subsequent work on this topic. The ITTC recommendations include the correction factor method of Stern [3] as well as the GCI.

The resolution to which the physics of a given problem are solved will determine the extents of the stochastic range, where some degree of scatter is present in solutions for varying grid refinement. When flow features are sufficiently resolved, the simulation will converge asymptotically with further grid refinement. CFD verification methodologies are derived from the work of Richardson [4], who identified the asymptotic approach to a continuum solution for finite difference calculations with increasing grid refinement.

In an attempt to overcome the vagaries of uncertainty estimation for CFD simulations, the following methodology is adopted [5]:

1 Uncertainty estimates are calculated (when possible) according to the methods described below, for multiple sets of grids.

2 The estimates are averaged and combined with the variance to represent scatter in results.

Grid Convergence Index

The so-called Richardson extrapolation was adopted by Roach [6] to estimate the uncertainty due to spatial and temporal errors in CFD.

(1)

Beginning with the generalized Richardson extrapolation:

$$f_0 \cong f_1 + \frac{f_1 - f_2}{r^p - 1}$$

$r = \frac{h_2}{h_1}$ is the grid refinement ratio for a characteristic grid height h. This is an expression for the function value at zero-grid spacing, based on the function value at a series of geometrically similar grids. The exponent p is either the theoretical or observed order of convergence. The difference $\delta_{RE} = f_0 - f_1$ is an estimate of the error for grid one, corresponding to a 50% uncertainty band when this value is interpreted as a single realization of that error. Thus:

(2)

$$U_{50\%} = \delta_{RE} = \frac{f_1 - f_2}{r^p - 1} \tag{3}$$

One might argue that δ_{RE} is derived from multiple realizations of the function: $f_1,\ f_2$. Finally, to extend the confidence interval to 95% Roach defines the Grid Convergence Index (GCI) as:

$$GCI = F_s * |\delta_{RE}|$$

F_s is interpreted as the coverage factor or, in engineering parlance, as the factor of safety. Roach suggests $F_s = 3$ for rudimentary grid convergence studies involving two grids, and $F_s = 1.25$ for more rigorous studies.

The efforts of Roach have been carried farther by Eca [7] [8], who has applied a least-squared approach in order to learn to accommodate scatter. Eca also incorporates the error estimates of Oberkampf [9], when data scatter is such that reliable estimates for the order of convergence, p, are not feasible. In these cases, convergence is assumed to proceed with either first or second order, or with mixed order.

(4)

(5)

(6)

$$\delta_1 = ch$$

$$\delta_2 = ch^2$$

$$\delta_{12} = c_1 h + c_2 h^2$$

Also, Eca introduced a weighting within the least squared minimization that favors the fine-grid solutions. Recognizing that practical ship flows CFD applications preclude the true approach to the asymptotic range while using three systematically refined grids, Eca proposes a weighting equal to the reciprocal of the characteristic grid height.

A selection is made among the available error estimates based on the observed order of convergence and the standard deviation for each fit. For cases where p is much greater or less than the expected order of convergence, the power-series estimate according to Oberkampf

that best fits the data is selected, with an increased $F_s = 3$. Once the error estimate has been selected, it is used to determine the uncertainty by considering the data scatter, Δ_ϕ, the degree to which the data behavior conforms to the error estimator (standard deviation of the fit), and the difference between the data value and the fit. A full description of this procedure is given in Eca [7].

(7)

$$\text{GCI} = \begin{cases} \boldsymbol{F_s\delta_i + \sigma + \left|\phi_i - \phi_{fit}\right|} & \boldsymbol{\sigma < \Delta_{phi}} \\ \boldsymbol{3\sigma/\Delta_\phi\left(F_s\delta_i + \sigma + \left|\phi_i - \phi_{fit}\right|\right)} & \boldsymbol{\sigma \geq \Delta_{phi}} \end{cases}$$

Correction Factor

In a parallel development, Stern and Wilson [10] have proposed an adaption to the Richardson extrapolation that assigns weights according to the observed order of convergence. This correction factor method is presented alongside the GCI of Roach in the ITTC recommended practices for CFD simulation verification [1]. The correction factor may be interpreted as an elaborated safety factor. The correction factor compares the observed rate of convergence with the theoretical order for the simulation and as a measure of the proximity of the grids used to the asymptotic range.

(8)

$$C = \frac{r^p - 1}{r^{p_{est}} - 1}$$

Where r and p are determined from a set of grids using the least-squares approach technique. If the observed order, p, is equal to the estimated order then C Is unity. For solutions outside the asymptotic range ($C \neq 1$), the sign and magnitude of C is used determine the uncertainty according to:

(9)

$$U_C = \begin{cases} [9.6(1-C)^2 + 1.1]|\delta_{RE}| & |1-C| < 0.125 \\ [2|1-C| + 1]|\delta_{RE}| & |1-C| \geq 0.125 \end{cases}$$

The final form of equation (17) has developed as a product of communications between Stern et al. [3] [10] and Roach, the product of which being that these approaches exhibit comparable behavior. For example, for the limit as $C \to 1$, $U = 1.1|\delta_{RE}|$.

Approximate Error Scaling

In a series of publications, [5] [11] [12], I. Celik has advanced the Approximate Error Scaling (AES) method for quantifying the uncertainty of CFD simulations. The premise of this approach is that the error at grid level i is proportional to the approximate error, a function for the change in simulation value with successive grid refinement. Similar to the construction of the error within the GCI formulations, the extrapolated relative error (ERE) is defined:

(10)

$$ERE = \left|\frac{\phi_0 - \phi_i}{\phi_0}\right|$$

The quantity $|\phi_0 - \phi_i|$ is estimated using a power series expansion for (αh), wherein the reciprocal of the refinement ratio $\alpha = \frac{1}{r}$ is used. A set of successively refined grids has the characteristic lengths $[h_1, h_2, h_3]$ such that $\alpha^2 h_1 = \alpha h_2 = h_3$. The expansion reads:

$$\phi(\alpha h) = \phi(0) + a_1(\alpha h) + a_2(\alpha h)^2 + a_3(\alpha h)^3 + h.o.t. \quad (12)$$

$$E_e(\alpha, h) = \phi(\alpha h) - \phi(0) = \sum_{k=1}^{\infty} a_k \alpha^k h^k$$

Defining also the approximate error E_a as the change in simulation value for progressive grid refinement by factor α:

$$E_a(\alpha, h) = \phi(\alpha h) - \phi(h) = \sum_{k=1}^{\infty} a_k(\alpha^k - 1)h^k \quad (13)$$

Finally, the extrapolated error, E_e is written in terms of the approximate error (as opposed to the numerical solution): (14)

$$E_e(\alpha, h) = \frac{1}{1 - \frac{\sum_{k=1}^{\infty} a_k h^k}{\sum_{k=1}^{\infty} a_k \alpha^k h^k}} E_a(\alpha, h)$$

The further evaluation of the right-hand-side is given in [5]. Finally, the data for a set of systematically refined grids is used to define a cubic spline for the extrapolated error (15) $E_a(\alpha, h)$. The associated uncertainty is estimated:

$$U_{AES} = 1.1 * ERE$$

The behavior for the approximate error (including its derivative), as h approaches zero, is additional information used in this method, over the input for methods based on the Richardson Extrapolation above. According to Celik, the exceptional performance of this method is attributed to this additional information about the behavior of the error in the limit for zero-grid size. [12]

GRID GENERATION

Simulation verification as described above requires a set of grids that are geometrically similar and cover a range of grid sizes within the asymptotic range. The definition if a set of grids is complicated by the unstructured nature of the FINE/Marine grid, and by the presence of boundary layer cells for typical ship flow simulations. Geometric similitude is achieved in the simplest sense by progressive subdivision of mesh cells. For three-dimensional problems, the resulting grids will exceed computing limits, and a compromise is necessary according to the available computational power. Particular interest in the sideforce generated by a ship with leeway angle, which is a product of massive flow separation and a wake of vortical structures passing around the hull, has led to an emphasis on the refinement diffusion when compromise was needed. For unstructured mesh generation with Hexpress, the refinement diffusion is doubled with each grid refinement.

The viscous layers, which must satisfy physical modeling requirements and cannot be scaled with the grid, will disrupt grid similitude. Some compromises were needed to construct the (11) meshes while satisfying the requirements of the log-law wall model. The wall normal cell

height was determined first by the analytic turbulent boundary layer height formula. Simulation results were used refine the first cell height to maintain $30<Y^{+}<100$ in so far as possible. Due to the recirculation region near the transom, Y^{+} values smaller than 15 were present for approximately 1.5% of the hull wetted surface. The maximum Y^{+} along the leading bilge was considered to be the driving consideration, as separation is expected at that location.

Systematic grid refinement is achieved by varying the initial cell subdivision and the refinement diffusion. The refinement levels for the hull and free surface are held constant. To conserve cells, cells at the hull are elongated to an aspect ratio of four along the X-axis. The free surface is captured with two refinement zones with a z-dimension equal to $L_{WL}/1000$. The wake of the ship is resolved with X- and Y- refinement equal to $L_{WL}/100$. Simulations are carried out at model scale, giving a relatively low Reyold's number of 2.3E6. This resulted in a first layer thickness that quickly satisfied the requirements of the log-law wall model with increasing grid refinement (see table XXX for information about grids). Still, as practical simulations will likely be performed using grids with viscous layers, these are included and marked with "vl" in table XXX. For grid 2, the compromise between cell height and diffusion refinement is apparent in the cell height, which is larger than desired for Y^{+}.

Mesh	Number of Cells N	Refinement Diffusion	h_{vol}	Initial Cell Height	Number of Viscous Cells	Mean Y^{+} (max)
1	8.8E+06	10	0.44	3.22E-03	-	40.8(84)
2	2.6E+06	5	0.65	4.79E-03	-	53.1(110)
2vl	2.0E+06	5	0.71	4.29E-03	2	42.5(84)
3	1.4E+06	3	0.81	4.29E-03	-	53(117)
3vl	1.1E+06	3	0.88	4.29E-03	5	52.2(86)
4	8.8E+05	2	0.94	4.29E-03	-	51(114)
4vl	7.3E+05	2	1.00	4.29E-03	5	60.4(93)

Table 1 – Details of Mesh Construction

An unstructured mesh for three-dimensional, complex geometries requires a definition for grid size. This dimension must be a length that is descriptive of the grid, and should decrease monotonically for a set of grids, preferably with constant refinement ratio r. Roach suggests the following: (16)

$$h_{vol} = \sqrt[3]{\frac{vol}{N}}$$

In which vol is the volume of the computational domain and N the number of cells. This definition for cell height is global quantity: it does not reflect the distribution of cells throughout the domain according to the refinement diffusion, which is of particular importance for capturing flow structures around the hull. In fact, an alternate definition for h that incorporates the (reciprocal of) refinement diffusion would be viable. As a consequence

of this ambiguity in the cell height metric, the observed order for the power-law fit should be interpreted with caution.

TURBULENCE MODELING

The task of modeling large-scale turbulent structures removed from the hull, such as separated bilge vortices, may challenge the assumptions made when averaging the Navier-Stokes equations. However, with the premium placed on economical simulations, it is considered impractical to include large-eddy simulation in the routine evaluation of hull variants. It is understood that flow around the hull will include large anisotropic vortices that will play a key role in the sailing performance of the hull. Turbulence is modeled with the Explicit Algebraic Stress Model (EASM), providing a balance between the Boussinesq-modeling and the modeling of Reynolds stresses and giving a more physical approach while remaining viable within the scope of work and for the computational resources available.

VERIFICATION CASES

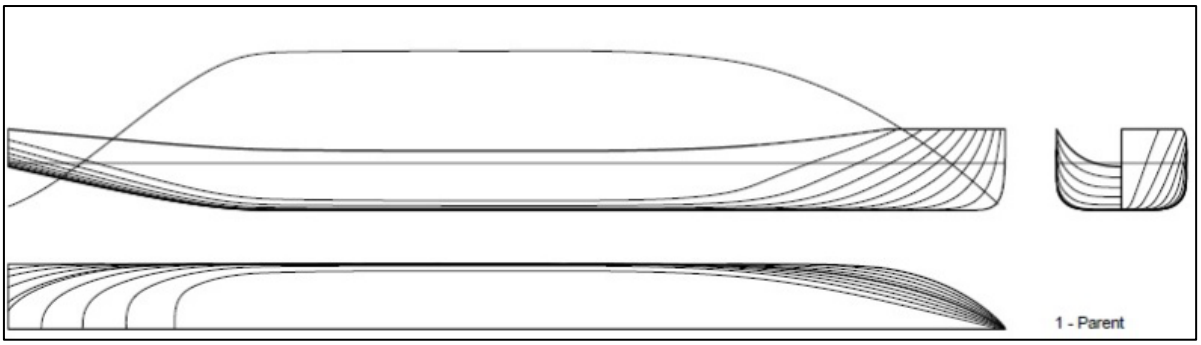

Figure 1 – Line plans for verification case

The parent hull of the 1st wind-assist systematic series is used for this verification exercise. The lines plan for the bare hull is given in figure 1. The simulation is performed at Fn=0.168, equivalent to 12 knots at full scale, and at 0, 9, and 20 degrees leeway. In total, 21 calculations were performed on 7 grids. Integrated fluid forces on the model are determined in the coordinate system aligned with the direction of forward motion.

Two grid subsets are defined as [1,2,3,4] and [1,2vl,3vl,4vl], so that the first set does not contain any viscous layers. The first set of grids exhibits smoother convergence behavior for sideforce and moment, and correspondingly, a better estimate of the uncertainty. Finally, the results for the two grid sets are averaged. Results for 9^o leeway are presented in detail.

Mesh	GCI	U_C	U_{EAS}	$\bar{U}$	σ_U	U_{X9}
1	0.4		2.8	1.6	1.7	3.3
2vl	4.9		4.7	4.8	0.1	4.9
3vl	6.9		6.1	6.5	0.6	7.0
4vl	17.8		16.4	17.1	0.9	18.0

Table 2 – Relative uncertainty estimates for resistance (9^o leeway)

The uncertainty for resistance is computed using the viscous-layer grids. The observed order of convergence was 6.5, resulting in exaggerated values for U_C, which have been omitted. For this case and for the yaw moment (table 4), the GCI formulation switches to the power series expressions (Oberkampf [9]), implying that the observed order is no longer reliable for error estimates with the correction factor.

Mesh	GCI	U_C	U_{EAS}	**Mesh**	GCI	U_C	U_{EAS}	$\bar{U}$	σ_U	U_{Y_9}
1	0.4	1.2	2.5	**1**	2.9	4.1	10.0	3.5	3.4	7.0
2	2.5	3.0	5.1	**2vl**	9.3	14.0	15.7	8.3	5.7	13.9
3	4.8	5.0	6.2	**3vl**	14.3	22.0	14.5	11.2	7.0	18.1
4	7.0	6.9	6.8	**4vl**	19.4	30.2	17.3	14.6	9.5	24.1

Table 3 – Relative uncertainty estimates for sideforce (9^o leeway)

Mesh	GCI	U_C	U_{EAS}	**Mesh**	GCI	U_C	U_{EAS}	$\bar{U}$	σ_U	U_{N_9}
1	10.3		3.7	**1**	8.4		6.2	7.1	2.8	10.0
2	12.2		7.0	**2vl**	10.9		10.6	10.2	2.2	12.4
3	11.8		8.0	**3vl**	11.6		12.0	10.9	1.9	12.8
4	11.3			**4vl**	11.6			11.5	0.1	11.6

Table 4 – Relative uncertainty estimates for yaw moment (9^o leeway)

The uncertainty estimation for sideforce is compelling. The broad agreement among the uncertainty formulations and between the two sets of grids suggests that the derived values are reliable. The observed order of convergence for the grid set without viscous layers was 2.3, while for the vicous layer set it was 2.5. The influence of convergence behaviour on the uncertainty estimate is apparent. The results for yaw moment are also congruent, though some numerical issues arose due to the low observed order of convergence (p=0.6).

Finally, the analysis is extended to the case for 20^o leeway, where it is expected that the threshold between the stochastic and asymptotic range may shift as separated flow structures becomes larger and more energetic. In fact, the methods outlined in this paper do not succeed for the sideforce indicating that the modelling errors in the simulation are such that simulation convergence in not possible. Estimates for the uncertainty are tabulated below.

Mesh	U_{X_0}	U_{X_9}	U_{Y_9}	U_{N_9}	$U_{X_{20}}$	$U_{Y_{20}}$	$U_{N_{20}}$
1	0.5	3.3	7.0	10.0	2.8		22.3
2	2.6	4.9	13.9	12.4	7.9		27.4

3	8.6	7.0	18.1	12.8	11.3		28.0
4	24.0	18.0	24.1	11.6	17.0		28.8

Table 5 – Overview of numerical uncertainty estimates

CONCLUSION

The discretization uncertainty for integrated forces on the ship hull has been established for bare hull configurations. The verification exercise described herein is a needed prerequisite for the reliable assessment of hull-form variants using CFD simulations. The verification has been conducted with particular focus on the hydrodynamic sideforce, as a leading component of the hydromechanics of wind-assisted ships. Further steps in this work will include the validation for bare hull cases, and the simulation of the appended hull.

REFERENCES

[1] Internation Towing Tank Commitee, "Recommended Practices- Uncertainty Analysis in CFD Verification Proceedures," 2008.

[2] American Society of Mechanical Engineers, "Standard for Verification and Validation in Computational Fluid Dynamics and Heat Transfer," ASME, 2009.

[3] F. Stern, R. Wilson, H. . Coleman and E. Paterson, "Comprehensive Approach to Verification and Validation of CFD Simulations--Part 1: Methodology and Procedures," *Journal of Fluids Engineering,* pp. 793-810, 2001.

[4] L. Richardson, "The Deferred Approach to the Limit," *Transactions of Royal Society London,* vol. 226, pp. 299-361, 1927.

[5] B. Celik and J. Li, "Assessment of Numerical Uncertainty for the Calculations of Turbulent Flow over a Backward-facing Step," *Internaional Journal for Numerical Methods in Fluids,* vol. 49, pp. 1015-1031, 2005.

[6] P. J. Roach, "Quantification of Uncertainty in Computational Fluid Dynamics," *Ann. Rev. of Fluid Mechanics,* vol. 29, pp. 123-160, 1997.

[7] L. Eca and M. Hoekstra, "A Proceedure for the Estimation of the Numerical Uncertainty of CFD Calculations Based on Grid Refinement Studies," *Journal of Computational Physics,* vol. 262, pp. 104-130, 2014.

[8] L. Eca, V. Guilherme and M. Hoekstra, "Code Verification, Solution Verification, and Validation in RANS Solvers," *Proceedings ASME Conference ence on Ocean, Offshore, and Arctic Engineering,* 2010.

[9] W. L. Oberkampf, "A Proposed Framework for Computational Fluid Dynamics Code Calibration/Validation," *AIAA,* no. 94-2540, 1994.

[10] F. Stern, R. . Wilson and J. Shao, "Quantitative V&V of CFD Simulations and Certification of CFD Codes," *International Journal for Numerical Methods in Fluids,* vol. 50, pp. 1335-1355, 2005.

[11] I. Celik and O. Karatekin, "Numerical Experiments on Application of Richardson Extrapolation with Nonuniform Grids," *Journal of Fluids Engineering,* vol. 119, pp. 584-590, 1997.

[12] I. Celik, J. Li, G. Hu and C. Shaffer, "Limitations of Richardson Extrapolation and some Possible Remedies," *Journal of Fluids Engineering,* vol. 127, pp. 795-805, 2005.

[13] H. Coleman and F. Stern, "Uncertainties and CFD Code Validation," *Journal of Fluids*

Engineering, pp. 795-803, 1997.